Control of the iron-tris(2,2'-bipyridine) light-induced excited-state trapping via external electromagnetic fields

Marc Alías-Rodríguez* and Miquel Huix-Rotllant*

Aix-Marseille Univ, CNRS, ICR, Marseille, 13013, France.

E-mail: marc.alias-rodriguez@univ-amu.fr; miquel.huix-rotllant@cnrs.fr

1 IR and RAMAN spectra

The simulated IR and Raman spectra at TPSSh/LANL2DZ level.

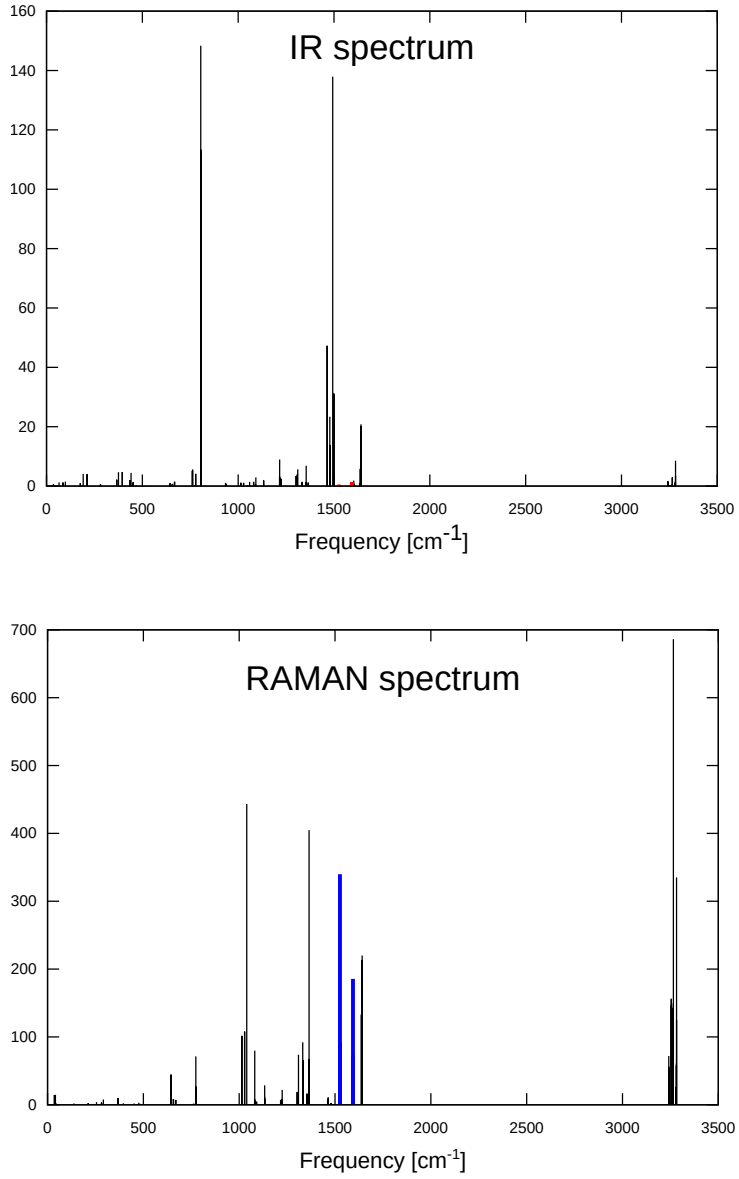

Figure S1: IR (top) and RAMAN (bottom) stick spectra at TPSSh/LANL2DZ level. The ligand modes included in the model Hamiltonian are marked in red for IR and blue for Raman spectra.

2 Radiation external field

The analytical shape of the chirped and non-chirped laser and their respective Fourier transform.

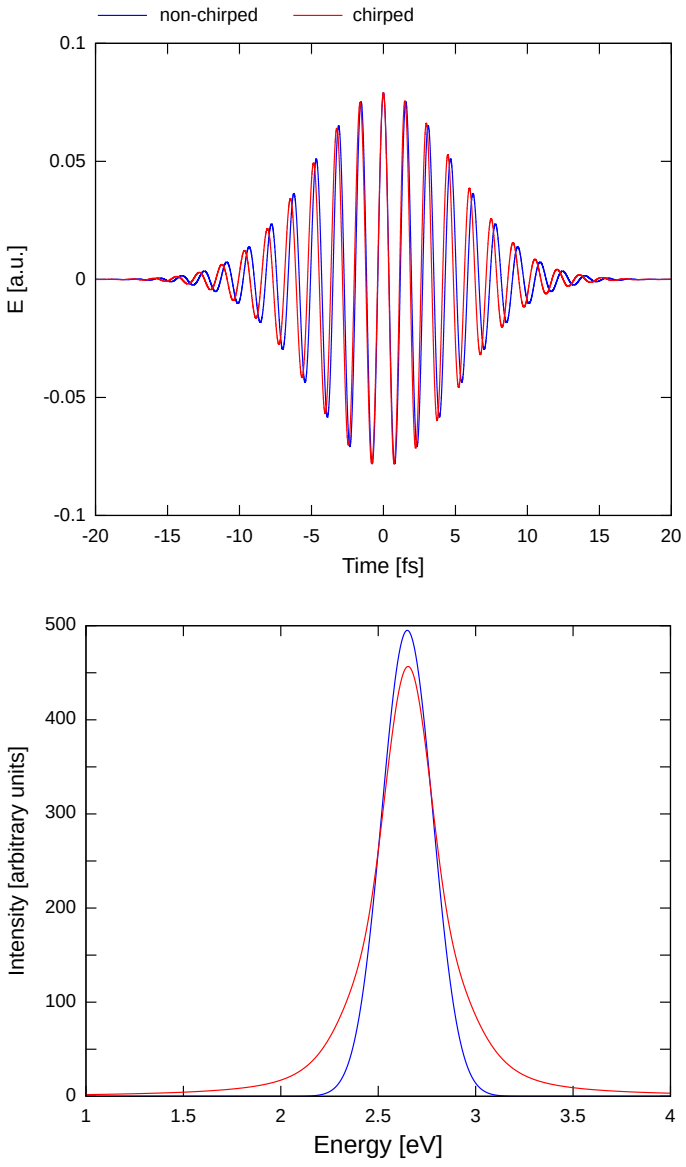

Figure S2: Time-evolution of the electric-field (top) and the corresponding discrete Fourier transform (bottom) using the non-chirped (blue) and chirped (red) analytical expression. The parameters employed have been those used in the model: E_0=0.079 a.u., σ=5.0 fs, T_0=1.56 fs, T_1=1.49 fs, T_2=1.63 fs and p_3=20 fs.

3 Gaussian-shaped electric field

Effect of the different analytical electric fields, i.e. chirped and non-chirped lasers.

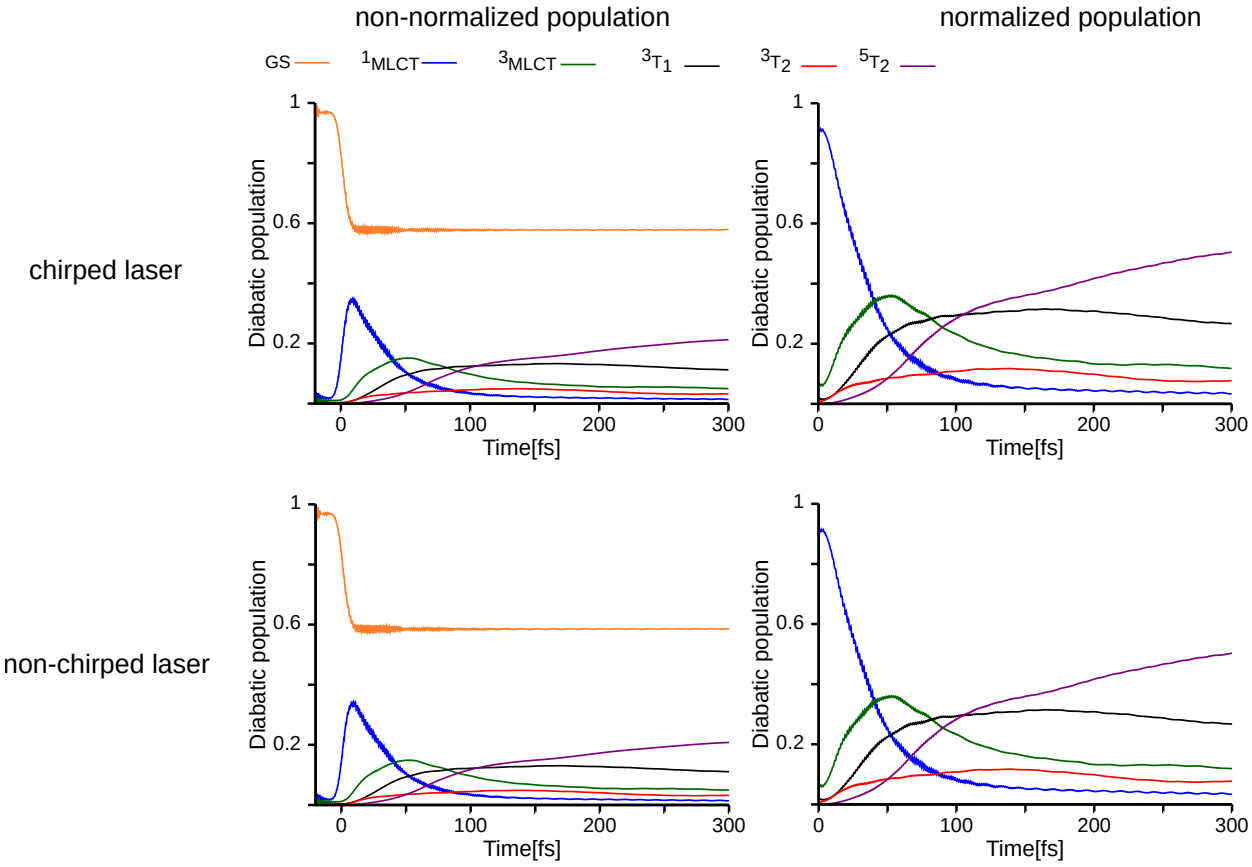

Figure S3: Time-evolution diabatic population. Ground state in orange, ^{1}MLCT in blue, ^{3}MLCT in green, $^{3}T_1$ in black, $^{3}T_2$ in red, and $^{5}T_2$ in pink. The left column graphs include the population on the singlet ground state and the right excludes this state. In the first row, the analytical expression for the electric field is the non-chirped cosine and in the second row, the laser electric field is chirped.

4 Effect of vibrational excitations

Evolution of the diabatic population for quantum dynamics initialized in the vibrationally excited states.

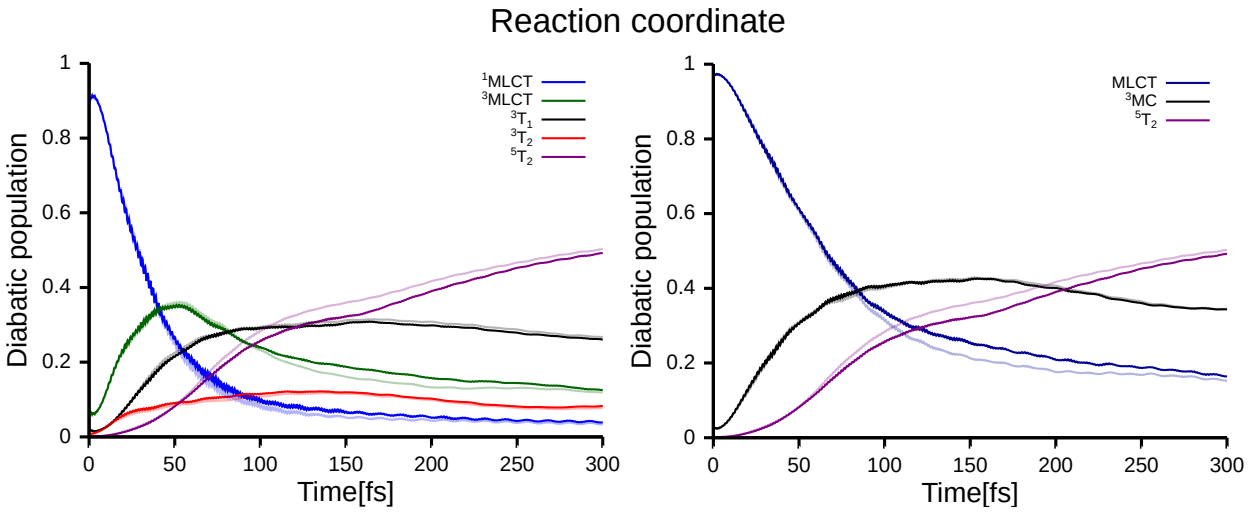

Figure S4: Time-evolution diabatic population from the vibrationally excited state v_{rc}=1 (solid lines) and from the vibrationally ground state (transparent line).

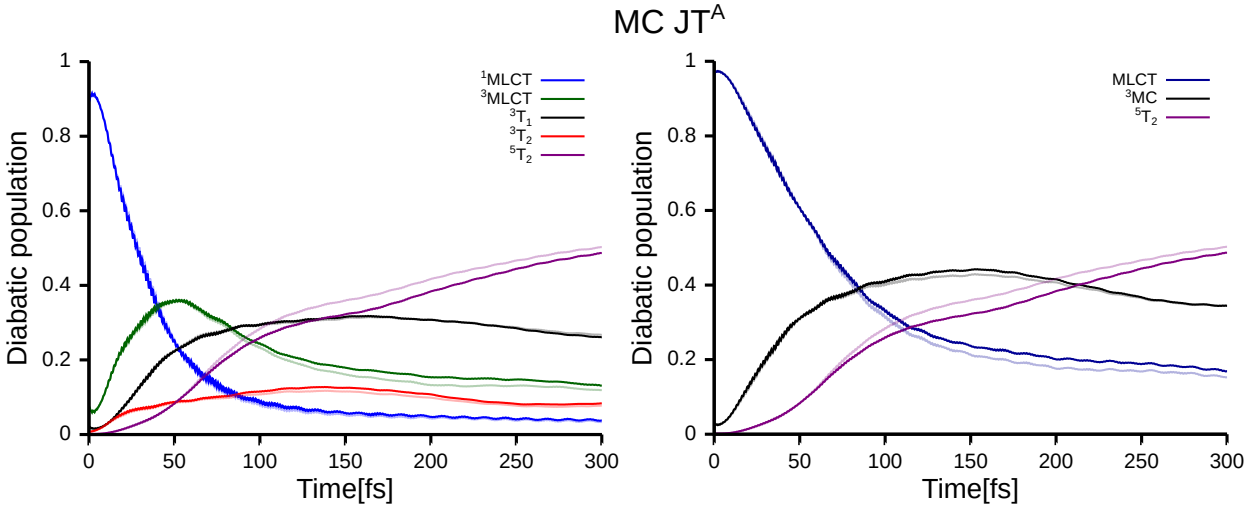

Figure S5: Time-evolution diabatic population from the vibrationally excited state v_{14}=1 (solid lines) and from the vibrationally ground state (transparent line).

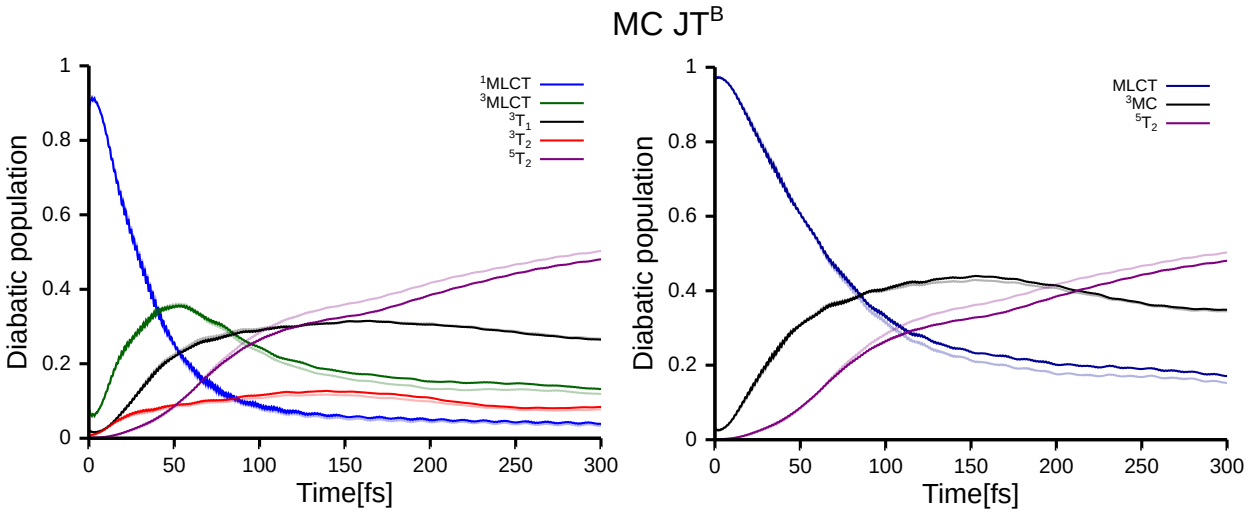

Figure S6: Time-evolution diabatic population from the vibrationally excited state v_{15}=1 (solid lines) and from the vibrationally ground state (transparent line).

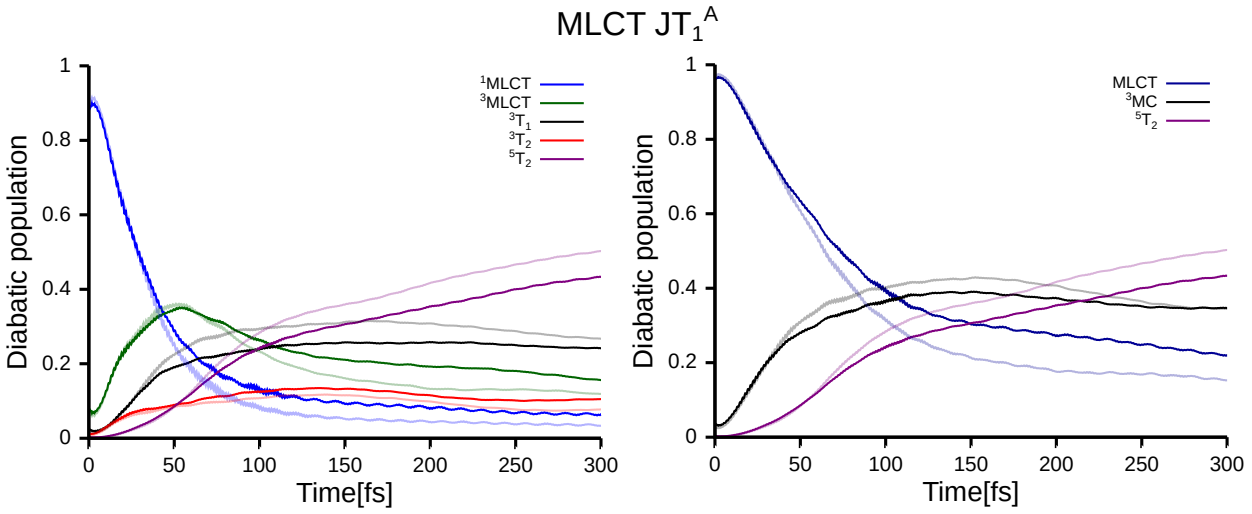

Figure S7: Time-evolution diabatic population from the vibrationally excited state v_{139}=1 (solid lines) and from the vibrationally ground state (transparent line).

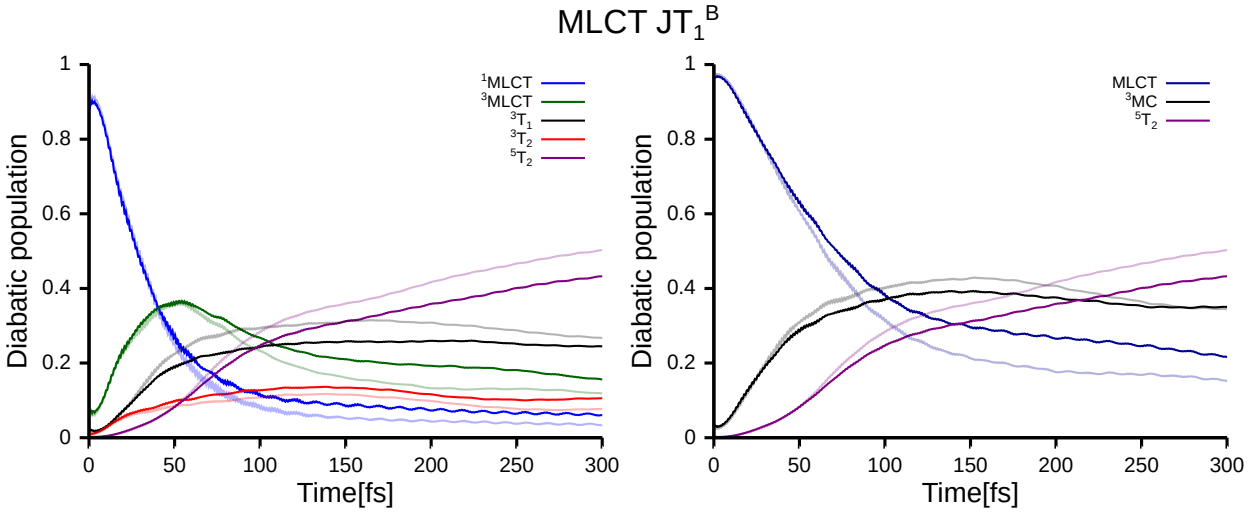

Figure S8: Time-evolution diabatic population from the vibrationally excited state v_{140}=1 (solid lines) and from the vibrationally ground state (transparent line).

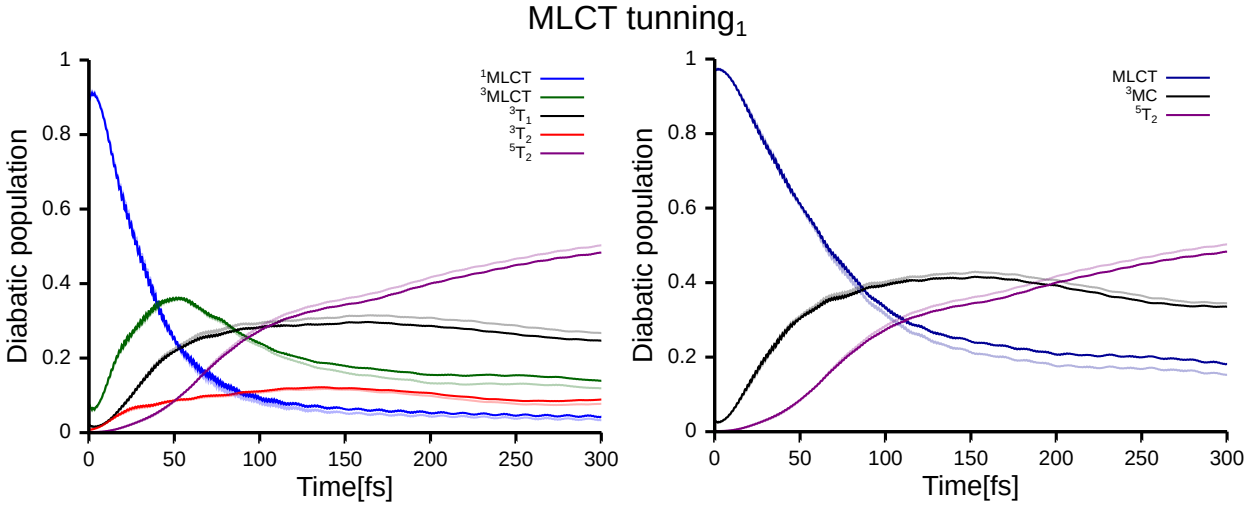

Figure S9: Time-evolution diabatic population from the vibrationally excited state v_{141}=1 (solid lines) and from the vibrationally ground state (transparent line).

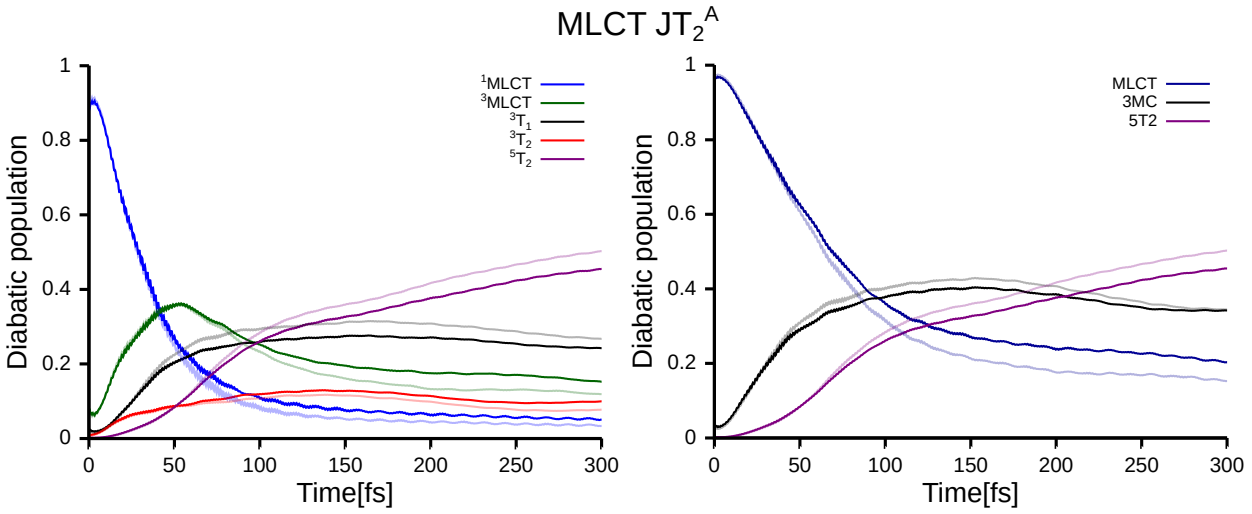

Figure S10: Time-evolution diabatic population from the vibrationally excited state v_{142}=1 (solid lines) and from the vibrationally ground state (transparent line).

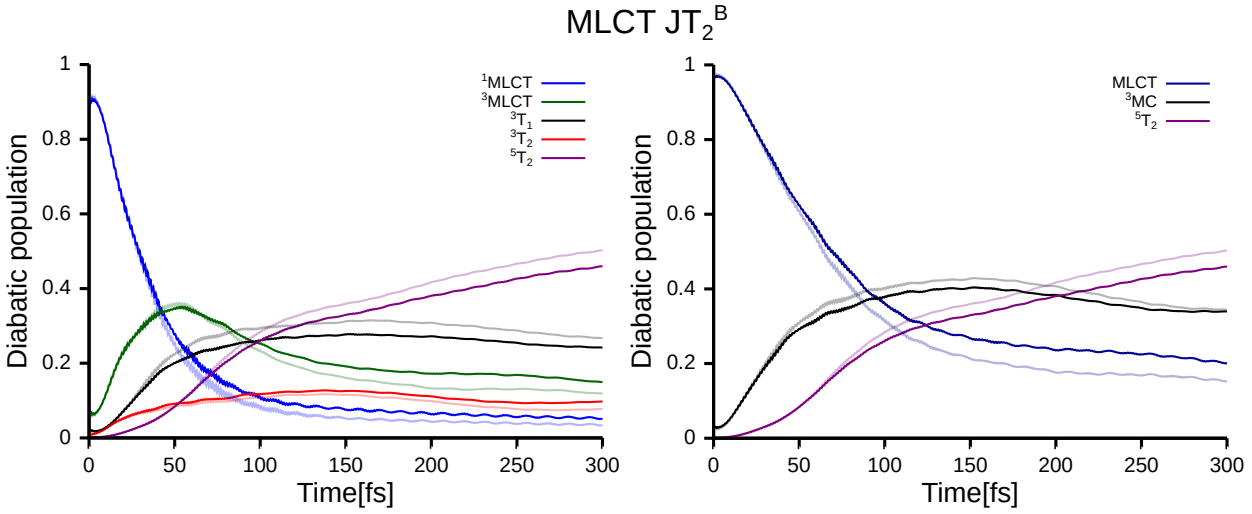

Figure S11: Time-evolution diabatic population from the vibrationally excited state v_{143}=1 (solid lines) and from the vibrationally ground state (transparent line).

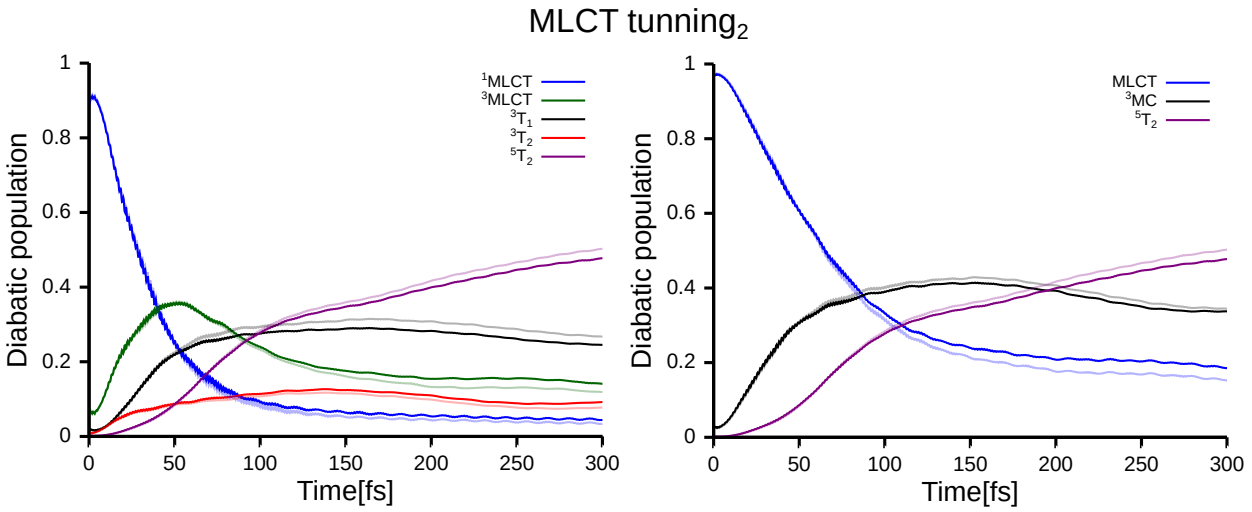

Figure S12: Time-evolution diabatic population from the vibrationally excited state v_{144}=1 (solid lines) and from the vibrationally ground state (transparent line).

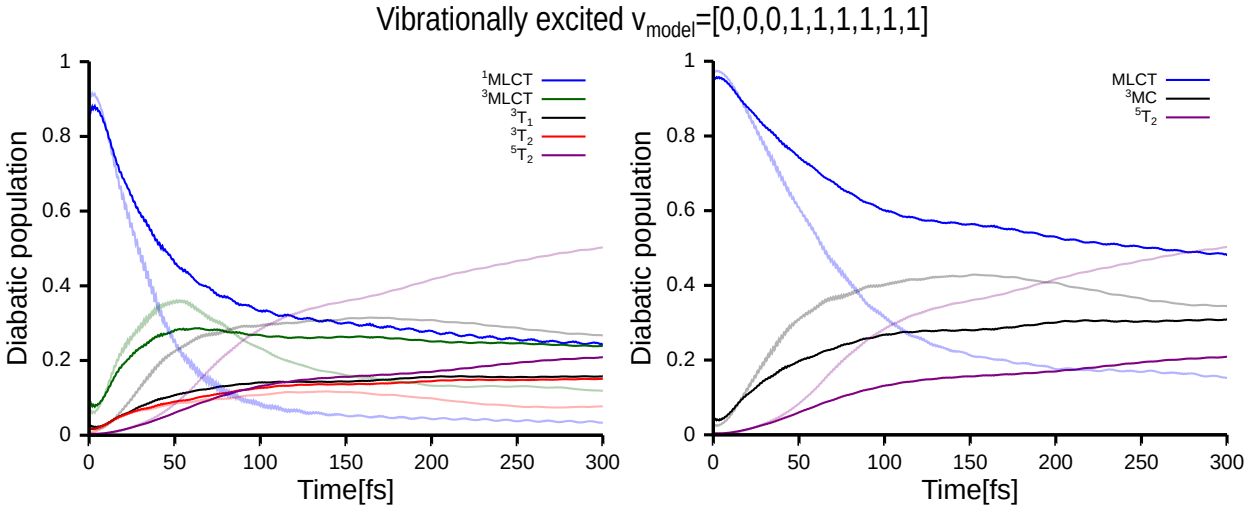

Figure S13: Time-evolution diabatic population from the vibrationally excited state v=1 for all the high-frequency modes (solid lines) and from the vibrationally ground state (transparent line).

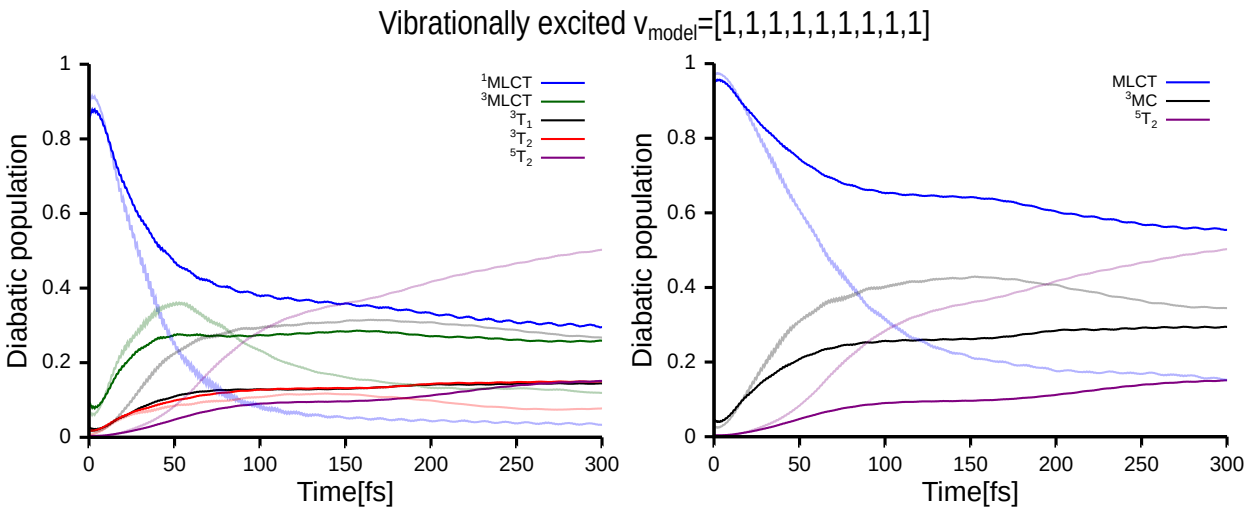

Figure S14: Time-evolution diabatic population from the vibrationally excited state v=1 for all the modes (solid lines) and from the vibrationally ground state (transparent line).

5 Optimal control laser

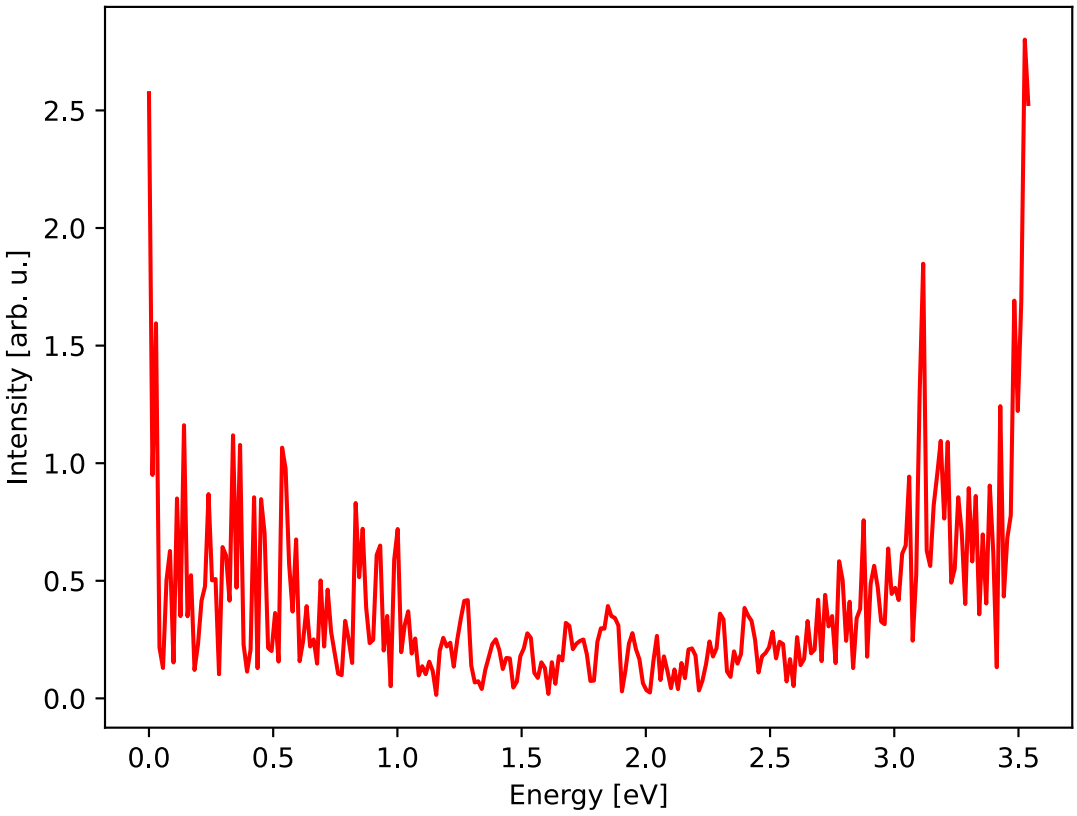

Figure S15: Fourier transform of the optimised laser.